Development ePress. Posted online 5 March 2014
© 2014. Published by The Company of Biologists Ltd | Development (2014) 141, 1-9 doi:10.1242/dev.101659

RESEARCH ARTICLE

microRNA-125 distinguishes developmentally generated and adult-born olfactory bulb interneurons

Malin Åkerblom[1], Rebecca Petri[1], Rohit Sachdeva[1], Thies Klussendorf[1], Bengt Mattsson[1], Bernhard Gentner[2] and Johan Jakobsson[1,*]

ABSTRACT

New neurons, originating from the subventricular zone, are continuously integrating into neuronal circuitry in the olfactory bulb (OB). Using a transgenic sensor mouse, we found that adult-born OB interneurons express microRNA-125 (miR-125), whereas the pre-existing developmentally generated OB interneurons represent a unique population of cells in the adult brain, without miR-125 activity. Stable inhibition of miR-125 in newborn OB neurons resulted in enhanced dendritic morphogenesis, as well as in increased synaptic activation in response to odour sensory stimuli. These data demonstrate that miR-125 controls functional synaptic integration of adult-born OB interneurons. Our results also suggest that absence of an otherwise broadly expressed miRNA is a novel mechanism with which to achieve neuronal subtype specification.

KEY WORDS: microRNA, Neurogenesis, Olfactory bulb, Mouse

INTRODUCTION

The mammalian olfactory bulb (OB) contains two interneuron subpopulations of different temporal and spatial origin. The first population is generated only during embryogenesis and the early postnatal period from local OB progenitor cells (Lemasson et al., 2005; Vergaño-Vera et al., 2006). Generation of the second population starts in the early postnatal period and continues during adulthood. This population emerges from neural stem/progenitor cells (NSPC) located in the subventricular zone (SVZ). NSPC produce neuroblasts that migrate to the OB, where they differentiate to inhibitory interneurons (Doetsch et al., 1999). In the present study, these two populations of OB interneurons are termed, for simplistic reasons, developmentally generated OB (DG-OB) interneurons and adult-born OB (AB-OB) interneurons. These two populations are thought to regulate distinct functions in odour discrimination and can be distinguished by several physiological and morphological characteristics (Alonso et al., 2012; David et al., 2013; Imayoshi et al., 2008; Lemasson et al., 2005; Magavi et al., 2005). Still, the molecular factors that discriminate these two neuronal populations remain largely unknown.

[1]Laboratory of Molecular Neurogenetics, Department of Experimental Medical Science, Wallenberg Neuroscience Center and Lund Stem Cell Center, Lund University, 221 84 Lund, Sweden. [2]San Raffaele-Telethon Institute for Gene Therapy and Vita-Salute San Raffaele University, via Olgettina 58, 201 32 Milan, Italy.

*Author for correspondence (johan.jakobsson@med.lu.se)

This is an Open Access article distributed under the terms of the Creative Commons Attribution License (http://creativecommons.org/licenses/by/3.0), which permits unrestricted use, distribution and reproduction in any medium provided that the original work is properly attributed.

Received 23 July 2013; Accepted 10 February 2014

MicroRNAs (miRNAs) are small non-coding RNAs that mediate post-transcriptional gene regulation. microRNA-125 (miR-125) is the mammalian homolog of *lin-4*, the first discovered miRNA in *Caenorhabditis elegans* (Lagos-Quintana et al., 2002; Lee et al., 1993; Wightman et al., 1993). miR-125 is highly expressed in the mammalian brain and cell culture experiments have linked miR-125 to regulation of neuronal differentiation and regulation of synaptic strength and function (Boissart et al., 2012; Edbauer et al., 2010; Le et al., 2009). However, the *in vivo* role of miR-125 in the brain remains unexplored. In this study, we demonstrate that DG-OB interneurons represent a unique population of neurons in the adult mouse brain lacking miR-125 activity. Inhibition of miR-125 in AB-OB interneurons results in a more complex dendritic tree and an increased synaptic activation after odour stimuli. These results indicate that miR-125 plays a key role in regulating the functional properties of AB-OB interneurons.

RESULTS

Generation of miR-125 sensor mice

In order to examine miR-125 activity *in vivo* we generated, using lentiviral transgenesis, sensor mice that allow visualisation of miR-125 activity in the brain (miR-125.T mice). We have recently demonstrated this approach to be an efficient way to study miRNA-activity pattern *in vivo* at a cellular resolution (Åkerblom et al., 2012; Brown et al., 2007). The miR-125.T mice carry a negative GFP sensor linked to the miR-125 target sequence (LV.miR-125.T; Fig. 1A-C). Thus, when miR-125 is present in the cell, it will inhibit expression of the GFP transgene. On the contrary, cells lacking miR-125 will express GFP (Fig. 1C). As a control, we used LV.GFP mice that carry an identical transgene with the exception of the miR-125-target sequence (Åkerblom et al., 2012).

Analysis of the miR-125.T sensor mice revealed that the majority of cells in the adult brain express miR-125, as demonstrated by the lack of GFP expression (Fig. 1D; supplementary material Fig. S1). However, we detected three distinct populations without miR-125 activity, visualised by GFP expression: cells in the OB, in the islands of Calleja (IoC) and in the habenula (Fig. 1D,E and supplementary material Fig. S1). These cells displayed neuronal morphology and expressed the neuronal marker NeuN (Fig. 1F and supplementary material Fig. S1). This expression pattern is in contrast to control LV.GFP mice, which express GFP in all neurons, including these three regions (supplementary material Fig. S1). As miR-125 has been linked to neurogenesis (Boissart et al., 2012; Le et al., 2009), we focused our subsequent analysis of miR-125 function to the OB. Using LNA-qRT-PCR, we found levels of miR-125b, but not miR-125a, to be lower in the OB compared with other brain regions (Fig. 1G). Fluorescent *in situ* hybridization (FISH) confirmed high expression of miR-125b in the brain (supplementary material Fig. S1K,L). In the OB, numerous cells negative for miR-125 were found, especially in the mitral cell layer (MCL). Lack of miR-125

Development (2014) doi:10.1242/dev.101659

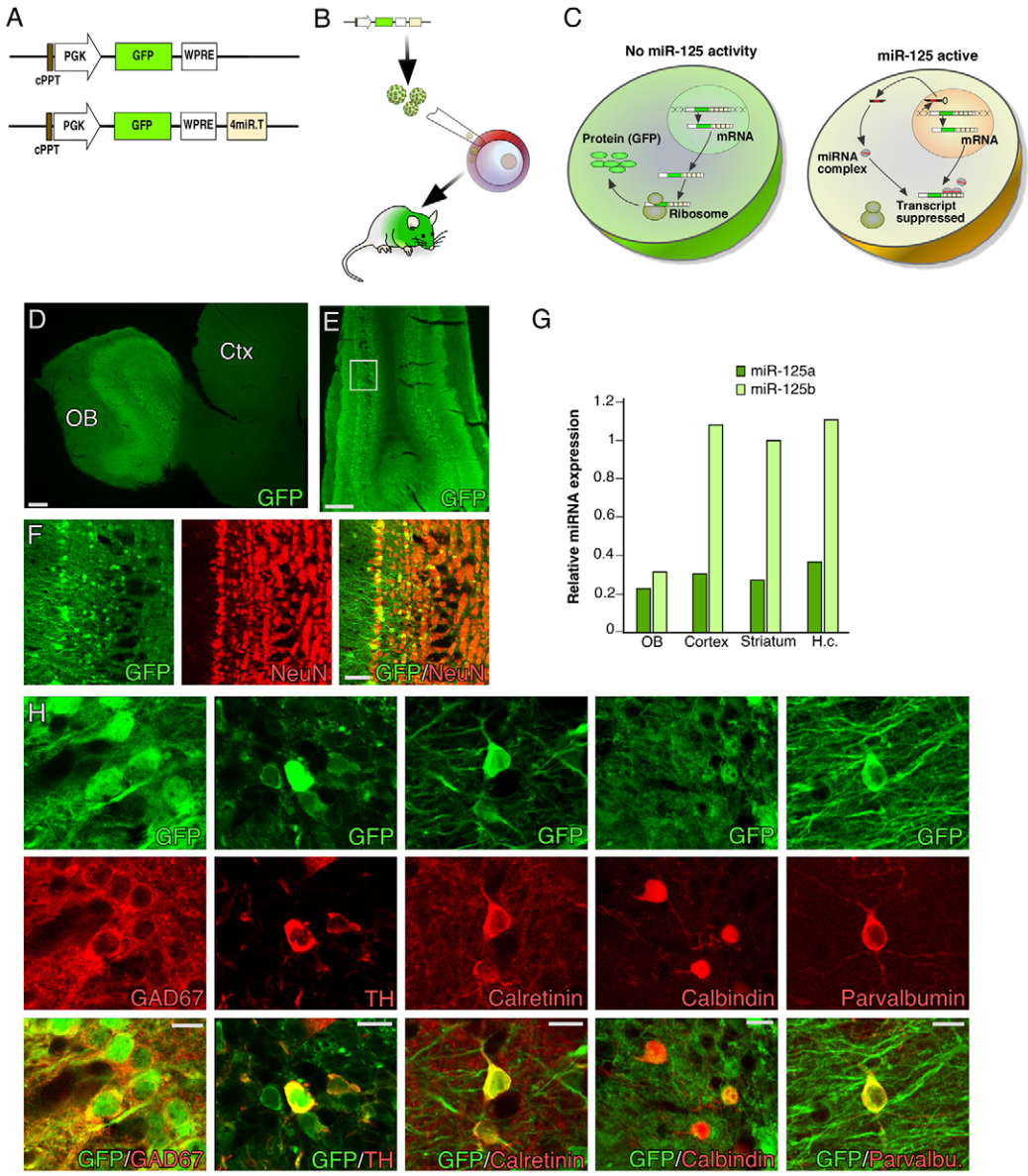

Fig. 1. Generation and characterisation of miR-125-sensor transgenic mice. (A) Illustration of the proviral form of LV.GFP and LV.miR-125.T. (B) Lentiviral transgenesis was used to generate the miR-125-sensor transgenic mice; lentiviral vectors were injected into the perivitaline space of fertilised embryos that were transferred to pseudopregnant females. (C) The miR-125-regulated lentiviral vectors are present in all cells of the transgenic animal. If no miR-125 is present in the cell, the vector is viable and GFP is expressed. By contrast, if miR-125 is present it binds and supresses the transgene, hence no GFP is expressed. (D) A sagittal section demonstrates lack of miR-125 activity in interneurons in the OB. (E) Coronal section of miR-125-negative cells in the OB. (F) miR-125 negative cells co-label with the neuronal marker NeuN. (G) LNA-RT-qPCR of miR-125b and miR-125a from OB, cortex, striatum and hippocampus shows that miR-125b levels but not miR-125a levels are lower in the OB compared with other brain regions. (H) Cells lacking miR-125 activity in the OB are heterogeneous interneurons corresponding to all major subtypes. PGK, phosphoglycerate kinase; GFP, green fluorescent protein; WPRE, woodchuck hepatitis virus post-transcriptional response element; cPPT, central polypurine tract; OB, olfactory bulb; Ctx, cortex; H.c., hippocampus. Scale bars: 250 µm in D,E; 25 µm in F; 10 µm in H.

was also noted in IoC, confirming the expression pattern found in the miR-125.T mice.

The miR-125-negative cells in the OB, which express GFP, appeared to be interneurons based on their morphology and their lack of axons extending outside of the OB (Fig. 1D-F). We found GFP-expressing cells belonging to the two main classes of OB interneurons: periglomerular cells (PGC) and granule cells (GC). Co-labelling with different subtype-specific markers, such as GAD67, TH, calretinin, calbindin and parvalbumin indicated that miR-125-negative cells (GFP-expressing) corresponded to all major subtypes of OB interneurons (Fig. 1H).

miR-125 negative interneurons are generated during development

We noted that the majority of miR-125 negative cells in the GC layer (GCL) were superficially placed (Fig. 1E,F). This positioning of GCs is similar to that reported for DG-OB interneurons (Imayoshi et al., 2008; Lemasson et al., 2005). We therefore hypothesised that miR-125 activity may separate this population from AB-OB interneurons. To probe this, we first performed bromodeoxyuridine (BrdU) birth-dating studies and injected the thymidine analogue into pregnant miR-125.T mice at embryonic day (E) 17.5 as well as into newborn miR-125.T mice at postnatal

Development (2014) doi:10.1242/dev.101659

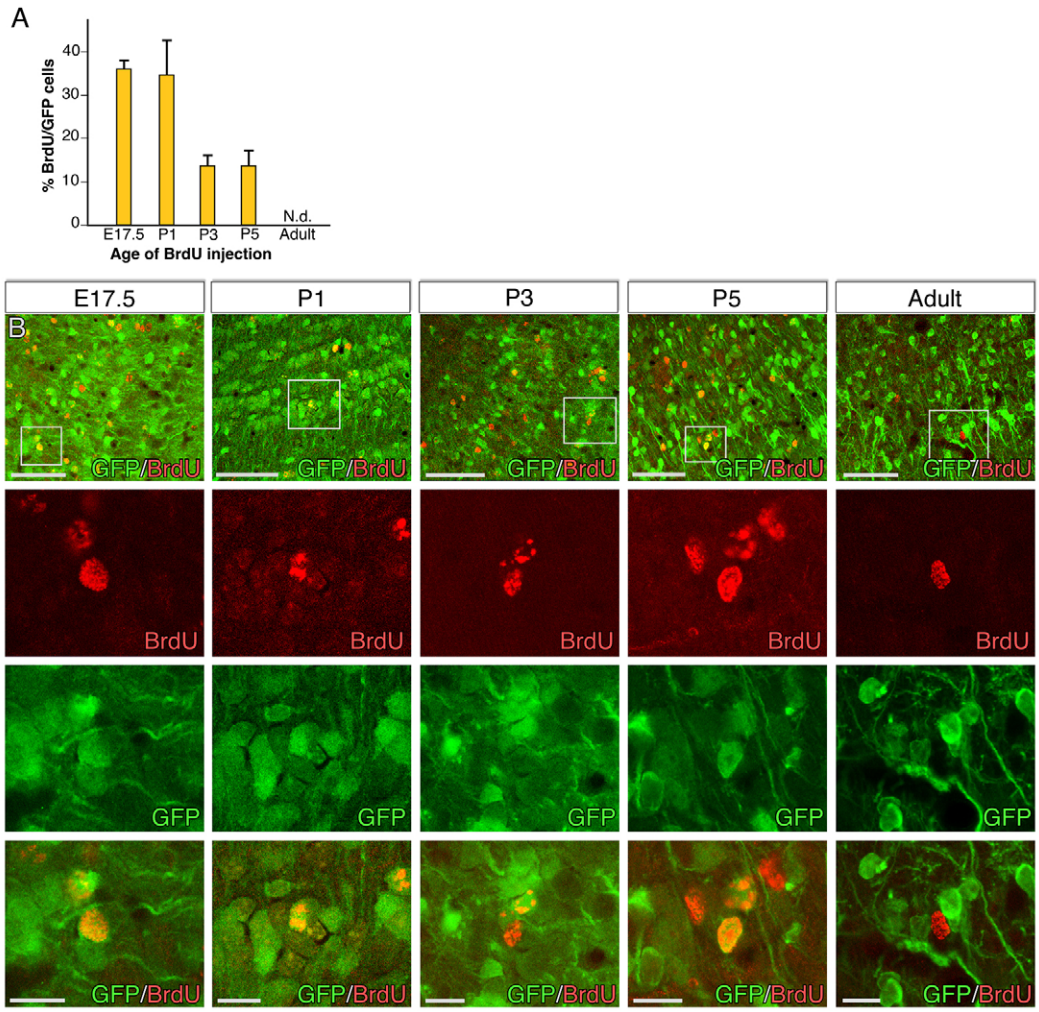

Fig. 2. Birthdating of miR-125-negative interneurons reveals a developmental origin. (A) BrdU injection at different ages and quantification of the number of GFP/BrdU double-positive cells in the OB, shows that most of the GFP (miR-125 negative) cells are born around E17.5-P1 and no GFP-positive cells are born during adulthood. Data are presented as mean±s.e.m. (B) Representative confocal images from the OB after the different time points of BrdU injection. Scale bars: 50 µm (top row); 10 µm (lowest three rows).

days (P) 1, 3 and 5. BrdU-injected animals were sacrificed at 4 weeks of age. We also injected BrdU into adult miR-125.T mice, which were sacrificed 4 and 6 weeks later. We found the highest proportion of BrdU/GFP double-labelled cells (around 35%) in animals receiving BrdU around birth (E17.5 and P1), whereas in animals injected at P3 and P5, the fraction of BrdU/GFP cells decreased (Fig. 2A,B). By contrast, when BrdU was injected in adult mice, we could not detect any GFP/BrdU co-labelled cells either 4 or 6 weeks after BrdU injection using confocal analysis (Fig. 2A,B; more than 100 BrdU-cells analysed by confocal microscopy). Thus, this experiment supports that miR-125 negative cells are DG-OB interneurons.

We confirmed this finding, using a second approach, by injecting a lentiviral vector (LV) expressing mCherry (LV.mCherry) into the lateral ventricle of P3 miR.125.T transgenic pups (Fig. 3A). We chose this experimental setup as it results in efficient labelling of the entire SVZ stem cell niche, including the NSPCs (Åkerblom et al., 2012). Transgene-labelled neuroblasts will subsequently migrate via the rostral migratory stream (RMS) and start to populate the OB around 2 weeks after LV injection, thus corresponding to the first wave of AB-OB interneurons cells. When we analysed LV-injected animals 4 and 8 weeks after injection, we found mCherry-expressing interneurons in the OB, often in close proximity to the GFP-expressing cells (miR-125-negative). Despite the similar positioning, we never detected GFP/mCherry double-labelled cells using confocal analysis (Fig. 3B; more than 100 mCherry-cells analysed by confocal microscopy).

Next, we wanted to investigate the position of the miR-125-negative cells in the OB of miR-125.T mice. Therefore, we injected wild-type P3 pups with a GFP control vector (LV.GFP) into the lateral ventricle to label AB-OB interneurons with GFP. We analysed the placement of GFP-expressing cells in the different OB cell layers in miR-125.T mice and compared the positioning to AB-OB interneurons labelled with LV.GFP at P3 in wild-type mice. LV-injected animals were analysed 4 weeks after vector injection. We found, in agreement with previous reports using BrdU labelling and genetic deletion (Imayoshi et al., 2008; Lemasson et al., 2005), that DG-OB interneurons are primarily found in the superficial GCL whereas AB-OB interneurons are primarily found deeper in the GCL (Fig. 3C,D). Taken together, these results demonstrate that, in the adult brain, interneurons lacking miR-125 in the OB are DG-OB interneurons and represent a separate cell population when compared with AB-OB interneurons that express miR-125.

Development (2014) doi:10.1242/dev.101659

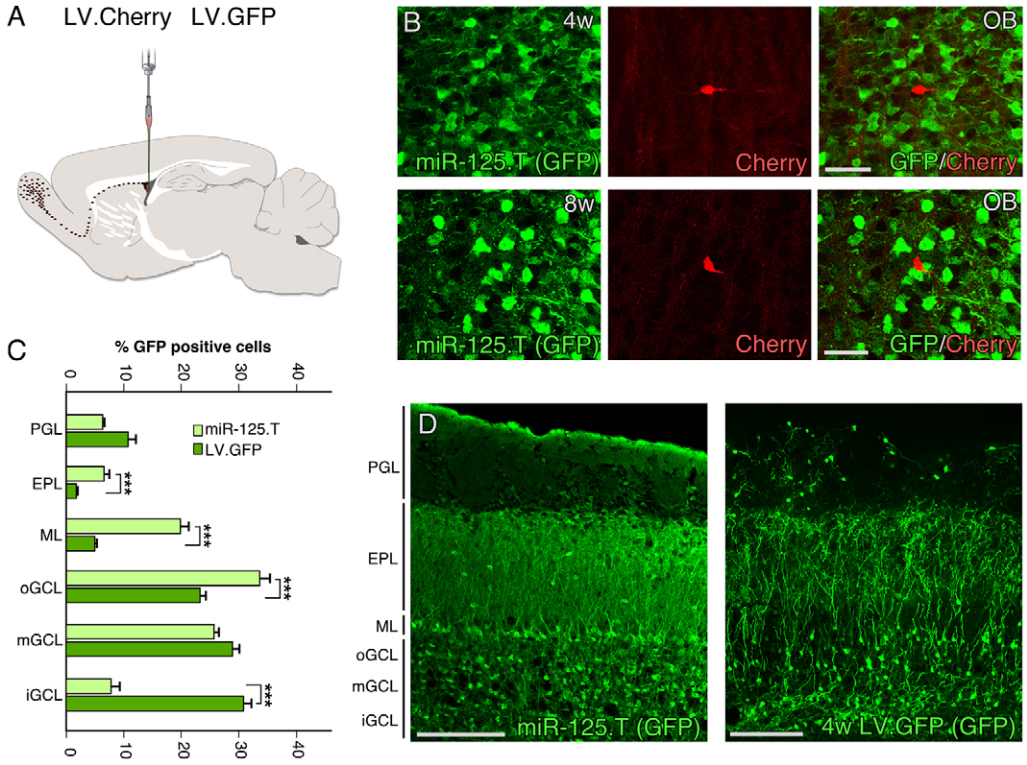

Fig. 3. miR-125-negative cells are developmentally generated and integrate in the superficial GC-layer. (A) Illustration of ventricular lentiviral vector injection (LV.Cherry, LV.GFP) at P3. (B) OB 4 and 8 weeks after LV.Cherry injection into the lateral ventricle of miR.125.T transgenic mice; no co-labelling of GFP and Cherry could be detected. Scale bars: 25 µm. (C) Quantification of GFP-expressing cells in the different cellular layers of the OB in miR-125.T mice and wild-type mice injected with LV.GFP in the lateral ventricle. Data are presented as mean±s.e.m. ***P<0.0001. (D) Representative images from the OB of miR-125.T mice and wild-type mice injected with LV.GFP in the lateral ventricle. Scale bars: 150 µm.

miR-125 regulates genes implicated in synaptic plasticity

The lack of miR-125 in mature DG-OB interneurons may, at least in part, explain the functional difference between this population and AB-OB interneurons. However, the functional role played by miR-125 in mature neurons is largely unexplored. We therefore decided to investigate genes regulated by miR-125 in neurons. To identify miR-125 targets, we used a previously published data set generated by using argonaute HITS-CLIP, a technique that allows the experimental identification of miRNA-mRNA interaction in specific cellular contexts (Chi et al., 2009). We used this data set to identify high-confidence miR-125-mRNA interactions in P13 mouse brain. We extracted all miR-125 targets where the binding site was located in the 3′UTR as this type of miRNA-mRNA interaction is most likely to cause transcriptional repression (Chi et al., 2009) (supplementary material Table S1). Functional annotation using DAVID bioinformatics analysis indicated that genes related to synaptic plasticity and synaptic functions are highly enriched among the 237 miR-125 target genes (Fig. 4A; supplementary material Table S2) (Huang et al., 2009). To experimentally validate this analysis, we selected 13 genes from the data set based on their functional classification and their HITS-CLIP cluster height. Using qRT-PCR, we confirmed that the majority of these genes are highly expressed in the OB when compared with other brain regions such as the hippocampus, which is the second neurogenic region in the adult brain, and the striatum (Fig. 4B). In addition, one of the potential miR-125 targets, *Map3k1*, was validated as a miR-125 target using a luciferase reporter assay (Fig. 4C). These data support the observation that, in neurons, miR-125 regulates genes related to synaptic functions.

miR-125 regulates dendritic morphogenesis of newborn neurons

We then performed loss-of-function experiments to investigate whether miR-125 regulates the formation of newborn AB-OB interneurons. In order to inhibit miR-125 activity stably in AB-OB interneurons, we generated a LV-sponge vector expressing eight copies of an imperfect miR-125 target sequence driven by a strong CMV promoter (LV.miR-125.sp, Fig. 5A). The functionality of LV.miR-125.sp was validated by the ability to de-repress transcripts that are known to be controlled by miR-125 (supplementary material Fig. S2). We injected LV.miR-125.sp vectors or GFP control vectors (LV.GFP) into the ventricle of wild-type P3 pups and analysed GFP expression 4 weeks later. The inhibition of miR-125 in the SVZ had no noticeable effects on neurogenesis and we detected numerous GFP expressing neurons in the OB, comparable with the GFP expression seen after LV.GFP injection (Fig. 5B). We then examined whether miR-125 regulates dendritic morphogenesis. Expression of LV.miR-125.sp resulted in a significant increase in total dendritic length and complexity compared with neurons expressing the control LV.GFP vector (Fig. 5C-G). No difference in the length of primary dendrites was found, suggesting that inhibition of miR-125 results in a more complex dendritic tree (Fig. 5F). Despite the increase in total dendritic length, inhibition of miR-125 had no effect on spine density, suggesting an increase in the absolute number of synapses on neurons expressing LV.miR-125.sp (Fig. 5H,I).

We then compared the positioning of newborn neurons expressing the LV.miR-125.sp and LV.GFP 4 weeks after vector injection in the different cellular layers of the OB. We found most newborn neurons in the GCL, regardless of miR-125 expression, showing that the inhibition of miR-125 does not change the placement of interneurons (Fig. 5J). Moreover, immunohistochemical staining for different interneuron markers, such as TH, calretinin and calbindin, revealed no difference in the formation of OB subtypes following miR-125 inhibition (data not shown). Collectively, these data show that miR-125 is important for the dendritic morphogenesis of newborn neurons. These results are in line with the gene ontology analysis of miR-125 target genes and support a role for miR-125 in regulating synaptic plasticity and neuronal integration.

Development (2014) doi:10.1242/dev.101659

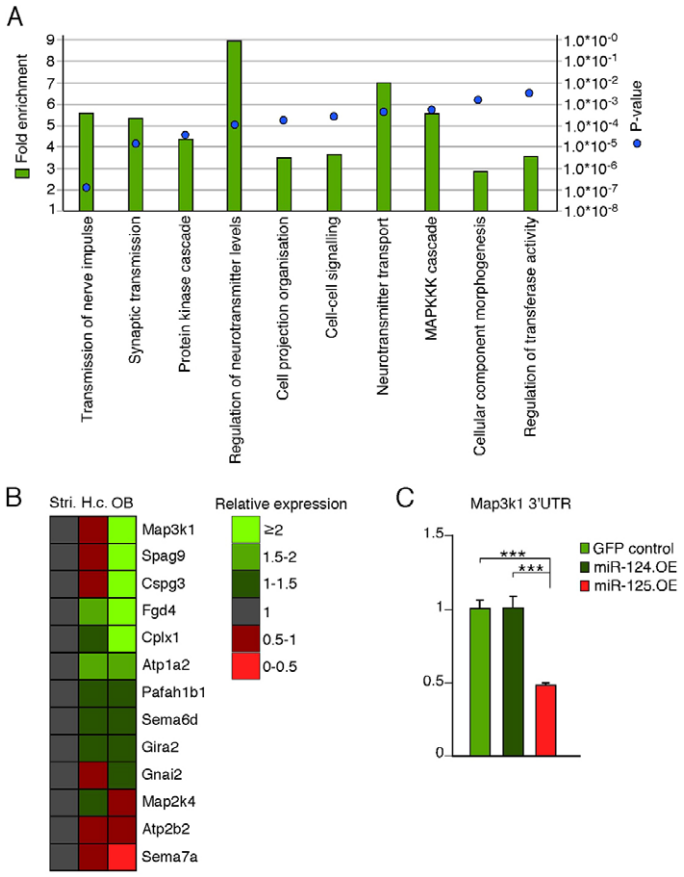

Fig. 4. miR-125 controls a large set of genes related to synaptic function. (A) DAVID bioinformatics database analysis showing Gene Ontology biological process classes of genes enriched in miR-125 target genes. The fold enrichment and *P* values are shown. (B) Heat map with qRT-PCR expression of 13 genes from the stri (striatum), H.c. (hippocampus) and OB. (C) Luciferase assay in 293 cells for the miR-125 target gene *Map3k1*. The luciferase reporter construct was co-transfected with a plasmid encoding miR-125, as well as with control constructs expressing GFP or the unrelated microRNA miR-124. Graph displays ratio of Renilla to firefly luciferase activity normalised to cells transfected with Map3k1-3′UTR only. Data represent mean of four independent experiments and are presented as mean±s.e.m.; ***$P<0.001$.

miR-125 controls functional integration of adult-born neurons

Adult born OB interneurons mature and integrate into circuitry over a period of several weeks. This process, which is remarkably slow compared with the time frame during development, is likely to be tightly controlled on a molecular level (Gheusi et al., 2013). To investigate whether miR-125 influences the functional integration of AB-OB interneurons, we assessed the expression of the immediate-early gene (IEG) *Fos* following odour stimulation. *Fos* is expressed as a result of electrophysiological activation and can be used to measure synaptic activation. Thus, analysis of *Fos* expression in the OB following odour stimulation allows simultaneous examination of the activity of thousands of adult-born and developmentally generated neurons following an environmental stimuli.

To inhibit miR-125 in adult-born OB neurons, we injected LV.miR-125.sp and control LV.GFP vectors into the RMS of adult mice. This results in efficient GFP labelling of migrating neuronal progenitors that will reach the OB 1 week later (Alonso et al., 2012). Three weeks after vector injection, mice were exposed to a battery of odours for 30 minutes, which is known to result in IEG activation, and were then immediately sacrificed (Fig. 6A).

In accordance with previous studies, we found a massive induction of *Fos* expression that was evenly distributed in GCL interneurons following odour stimulation (Carlén et al., 2002; Magavi et al., 2005). Odour exposure resulted in *Fos* expression in around 15% of all GCL OB interneurons whereas non-exposed mice demonstrated an almost complete lack of *Fos* expression (Fig. 6B). Quantification of Fos/NeuN in LV.GFP- and LV.miR-125.sp-injected animals demonstrated an equal level of odour activation for both conditions (Fig. 6C).

The lentiviral vector injections into RMS resulted in labelling of numerous adult-born OB neurons that could be monitored by GFP expression. As the mice were sacrificed 3 weeks after vector injection, the GFP/NeuN-expressing, AB-OB-interneurons will be 1-2 weeks old, and thus represent a population that have not yet reached full maturation and integration. In accordance with this, we found that newborn neurons labelled with the control LV.GFP vector displayed greatly reduced activation frequency when compared with the entire population of OB-interneurons identified by NeuN. Only 8% of LV.GFP labelled neurons co-labelled with Fos following odour stimulation, compared with 15% of the NeuN-population (Fos/NeuN) (Fig. 6C-E). Most interestingly, we found that AB neurons expressing the miR-125 sponge construct did not display this difference. Instead, we found that 14% of LV.miR-125.sp-labelled neurons co-labelled with Fos following odour stimulation, a similar activation frequency in adult-born cells when compared with the whole NeuN-expressing OB population (Fig. 6E). These data demonstrate that miR-125 controls functional integration of adult-born neurons as inhibition of miR-125 increases the activation of newborn neurons after odour stimulation. Thus, miR-125 expression may influence the slow, controlled integration of adult-born neurons, which is thought be essential for the unique functions of this population.

DISCUSSION

AB-OB and DG-OB interneurons differ in both their temporal and spatial origin. DG-OB interneurons are generated during embryogenesis and the early postnatal period, mostly from local OB progenitors (Lemasson et al., 2005; Vergaño-Vera et al., 2006). AB-OB interneurons, which are constantly added to the olfactory bulb during the postnatal period and adulthood, derive from progenitors located in the SVZ. Furthermore, AB-OB interneurons have several physiological and morphological characteristics that distinguish them from DG-OB interneurons. Although DG-OB interneurons persist throughout life, AB-OB interneurons are subjected to a constant turnover (Imayoshi et al., 2008; Lemasson et al., 2005). Integration of AB cells is targeted to specific regions of the OB, primarily the deep granule cell layer (GCL) (Imayoshi et al., 2008; Lemasson et al., 2005), and AB cells also have a tendency to generate certain subtypes of interneurons (Batista-Brito et al., 2008). In addition, AB neurons display distinct electrophysiological characteristics, including a tendency to display stronger sodium currents (Belluzzi et al., 2003) and a distinct immediate-early gene response to odour stimulation (Magavi et al., 2005). Thus, there is a large body of evidence demonstrating that developmental and adult neurogenesis produce distinct populations of OB interneurons, which are likely to mediate functional differences. The identification of miR-125 activity as a marker that distinguishes DG-OB and AB-OB interneurons from each other provides a molecular basis for the functional differences described between these cell populations.

Development (2014) doi:10.1242/dev.101659

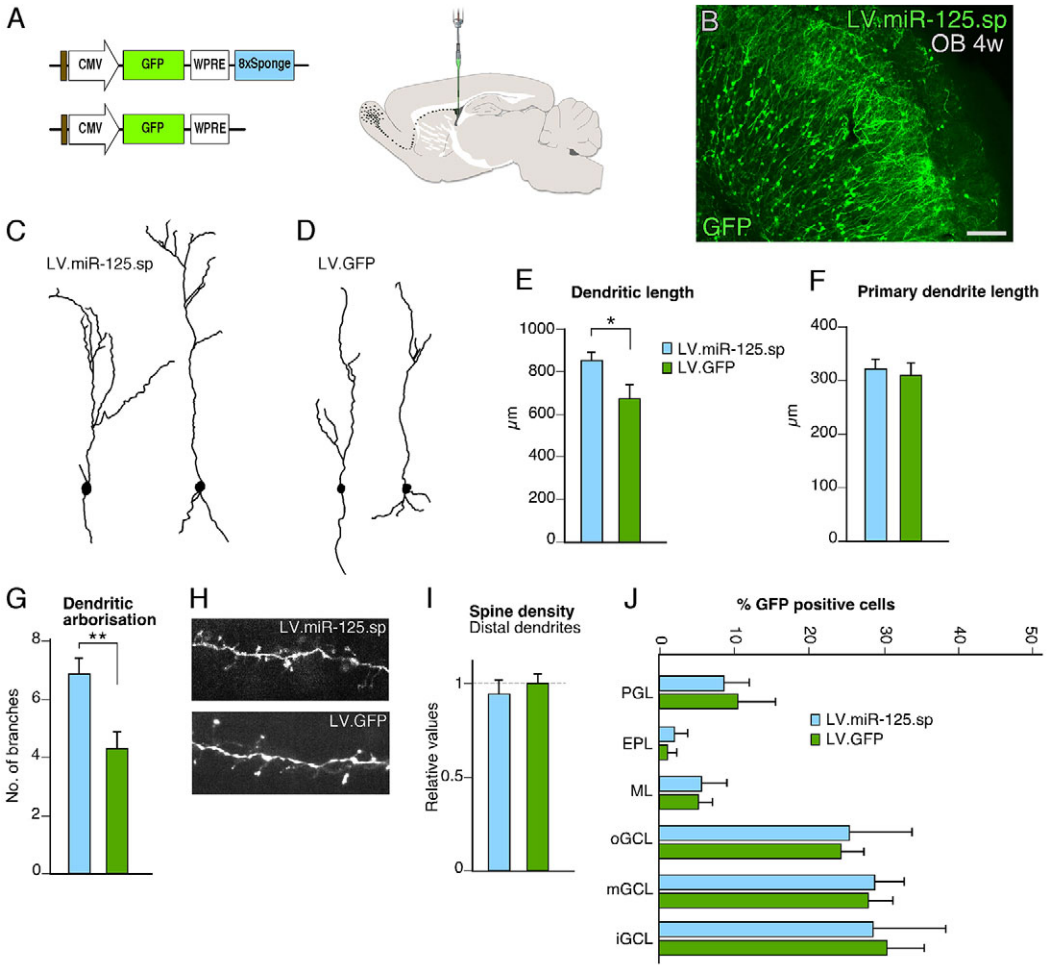

Fig. 5. miR-125 controls dendritic length and branch points of newborn GCL neurons, but not positioning. (A) Illustration of the proviral form of LV.miR-125.sp and LV.GFP, and the ventricular vector injection. (B) GFP expression in the OB 4 weeks after LV.miR-125.sp injection into the lateral ventricle of wild-type P3 pups. Scale bar: 100 µm. (C) Representative reconstructions of LV.miR-125.sp-expressing newborn neurons in the GCL, 4 weeks after vector injection. (D) Representative reconstructions of LV.GFP-expressing newborn neurons in the GCL, 4 weeks after vector injection. (E) Total dendritic length (µm) of LV.miR-125.sp- and LV.GFP-expressing newborn neurons in the GCL, 4 weeks after vector injection; **P*<0.05. (F) Length of the primary dendrite (µm) of LV.miR-125.sp- and LV.GFP-expressing newborn neurons in the GCL, 4 weeks after vector injection. (G) Dendritic arborisation presented as total number of branches in the dendritic tree of LV.miR-125.sp- and LV.GFP-expressing newborn neurons in the GCL, 4 weeks after vector injection; ***P*<0.01. (H) Representative images of spines of LV.GFP- and LV.miR.125.sp-expressing GCL interneurons. (I) Spine density of LV.miR-125.sp- and LV.GFP-expressing newborn neurons in the GCL, 4 weeks after vector injection, presented as relative to control. (J) Quantification of GFP-expressing cells in the different cellular layers of the OB in LV.miR-125.sp-injected mice 4 weeks after injection into the lateral ventricle. PGL, periglomerular layer; EPL, external plexiform layer, ML, mitral cell layer; oGCL, outer granule cell layer; mGCL, middle granule cell layer; iGCL, inner granule cell layer.

The identification of DG-OB interneurons was made possible by generating a GFP miRNA sensor mouse (Åkerblom et al., 2012; Åkerblom et al., 2013), which has the advantage that it allows visualisation of the activity of miRNAs at single-cell resolution. As the reporter system is inverted, the miR-125-negative cells are seen as GFP positive, which makes it possible to detect small, discrete populations of cells lacking miR-125, such as the DG-OB interneurons. By using BrdU birth labelling, we found that the miR-125-negative cells in the OB are born before or just after birth but not during adulthood, demonstrating that AB-OB interneurons express miR-125 whereas DG-OB interneurons do not. In addition, the pattern of transgene expression is similar to that previously reported for the positioning of DG-OB interneurons, i.e. with the majority of GFP-positive cells located in the superficial part of the GCL (Imayoshi et al., 2008; Lemasson et al., 2005). We also demonstrate that the spatial origin of postnatal-born GFP-expressing cells in the miR-125.T mice is not the SVZ, which is in line with the identification of miR-125 negative cells as DG-OB interneurons. When we labelled NSPCs in the SVZ at P3 using a mCherry-expressing viral vector, we were unable to co-label the GFP-expressing cells in the sensor mice.

To understand the functional role of miR-125, we used a previously published argonaute HITS-CLIP data set generated from mouse brain (Chi et al., 2009). This strategy allows the experimental identification of miRNA targets from specific cell populations. In our present study, we found using *in silico* analysis, that in the mouse brain, miR-125 regulates a large network of genes whose functional role is linked to synaptic mechanisms. The analysis of the HITS-CLIP data set suggests that miR-125 regulates over 200 genes. Thus, it is possible that a combination of target genes, rather than a single miRNA-mRNA interaction, is responsible for the functional consequence of miR-125 mediated repression. Future experiments aiming at profiling changes in both the transcriptome and proteome of OB interneurons following miR-125 perturbation will be very interesting.

Development (2014) doi:10.1242/dev.101659

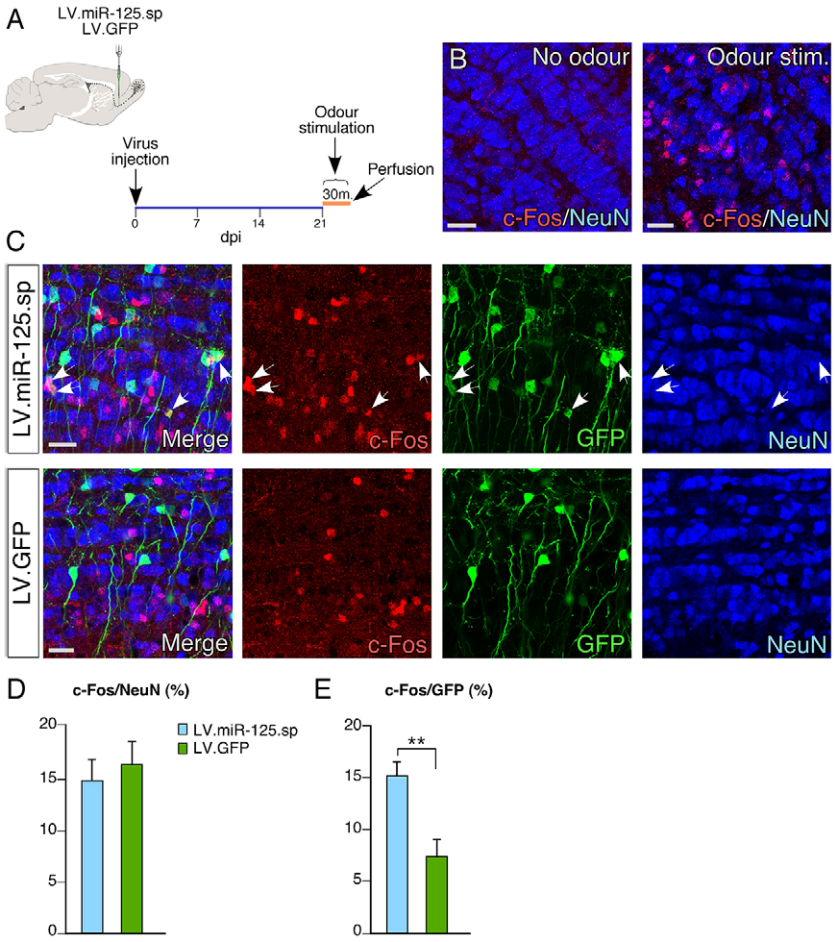

Fig. 6. miR-125 controls the functional integration of adult-born GCL neurons. (A) Illustration of the RMS injection of LV.GFP and LV.miR-125.sp and the experimental set-up. Twenty-one days after virus injection into the RMS, mice were exposed to a battery of odours for 30 minutes and perfused immediately after. (B) Odour exposure resulted in Fos-labelled cells in the OB. Scale bars: 20 µm. (C) Fos/GFP/NeuN staining of odour-exposed mice. LV.miR-125.sp-expressing cells (top row, arrowheads) display a higher proportion of triple-labelled cells compared with LV.GFP cells. Scale bars: 20 µm. (D) Fos/NeuN double-positive cells from LV.miR-125.sp- and LV.GFP-injected mice (%). (E) Fos/GFP double-positive cells from LV.miR-125.sp- and LV.GFP-injected mice (%); $^{**}P<0.01$. Data are presented as mean±s.e.m.

Our loss-of-function analysis using a miR-125 sponge vector confirmed the prediction from the *in silico* analysis and showed that the inhibition of miR-125 in newborn AB-OB interneurons is associated with enhanced dendritic morphogenesis. A more elaborate dendritic tree may receive stronger synaptic input from principal mitral cells. In line with these molecular and morphological findings, we indeed found that inhibition of miR-125 leads to increased activation of AB-OB interneurons, as demonstrated by increased Fos expression following odour stimulation.

Collectively, these data demonstrate that miR-125 plays an important role in regulating the integration of AB neurons into the OB circuitry. Our data also suggest that in the adult OB, miR-125 acts as a heterochronic gene that regulates the developmental timing of newborn neurons. miR-125 may promote the slow functional integration that occurs during adult neurogenesis by repressing genes related to synaptic functions. Although the functional role of AB-OB interneurons remains debated, there are several functional studies that point to a unique role of AB-OB interneurons in modulating olfaction (see, for example, Alonso et al., 2012; Magavi et al., 2005). In particular, the timing of integration of AB-OB interneurons appears to be crucial for their functional role in odour discrimination. Previous studies have found that both electrophysiological and functional properties of AB-OB interneurons change during the process when the newborn neurons mature and age (Gheusi et al., 2013). Our results point towards a key role for miR-125 in this process. An intriguing question that arises from our study is why do DG-OB interneurons require the unique synaptic properties they obtain by the lack of miR-125 activity? One possibility is that the absence of miR-125 facilitates the integration of newborn AB-OB interneurons that enter into the local network by increasing the probability of establishing synaptic contacts with pre-existing DG-OB interneurons. With this in mind it is interesting to note that we also find GFP-expressing cells in the island of Calleja in miR-125.T mice. Adult-born neurons originating from the SVZ have also been reported to integrate into this structure, albeit at a low frequency (De Marchis et al., 2004).

Finally, our data suggest that it is possible that the absence of activity of an otherwise broadly expressed miRNA, such as miR-125, is a more general mechanism to achieve neuronal subtype specificity. In line with this, we have recently found, using a similar sensor mouse strategy, that miR-9 is specifically absent from a few neuronal nuclei near the midline and in the hypothalamus (Åkerblom et al., 2013). Thus, lack of specific miRNA activity may be a way to achieve unique properties in a neuronal population. How the lack of miRNA activity is achieved remains unknown, but could be regulated at the transcriptional level or by post-transcriptional mechanisms including endogenous miRNA sponges (Hansen et al., 2013).

MATERIALS AND METHODS

Viral vectors

The lentiviral vectors used in this study were third-generation SIN vectors. miRNA target sequences were cloned into the 3′ untranslated region (UTR) of the transgene expression cassette. A detailed description on how to generate lentiviral vectors with miRNA target sequences has been described

Development (2014) doi:10.1242/dev.101659

elsewhere (Brown et al., 2007). The target sequence used in the sensor construct (miR-125.T) for miR-125b is TCACAAGTTAGGGTCT-CAGGGA (mirbase.org). The four target sites were cloned immediately downstream of the woodchuck hepatitis virus post-transcriptional response element (WPRE) of a third-generation lentiviral vector, expressing GFP from the PGK promoter derived from the phosphoglycerol kinase housekeeping gene. This promoter results in robust, ubiquitous moderate level transgene expression, with very low tendency to transgene silencing/variegation.

The miR-125 sponge vector contained eight repeats of an imperfectly complementary sequence forming a central bulge when binding to miR-125. The sponge was cloned into a third generation lentiviral vector containing a strong promoter derived from cytomegalovirus (CMV), a requirement for successful miR-125 inhibition. The miR-125.sp sequence is: TCCCTG-AGACTAAACTTGTGA. All cloning was performed using standard techniques. Lentiviral vectors were produced as previously described (Zufferey et al., 1997). Vectors were titrated using flow cytometry and quantitative RT-PCR analysis, as previously described (Georgievska et al., 2004). The titres of the vectors in this study were in the range of: 5×10^8-2×10^9 TU/ml.

Animals

All animal-related procedures were approved by and conducted in accordance with the committee for use of laboratory animals at Lund University and EPFL.

Lentiviral trangenesis was performed as previously described previously (Sauvain et al., 2008). Offspring were genotyped and number of integrated transgenes was estimated using quantitative RT-PCR. Primers are found in supplementary material Table S3. The data was quantified using the ΔΔCt-method. The transgene data (WPRE primer) was normalised with the Titine data to give the number of transgenes in the genome of each animal.

We generated eight transgenic founders all carrying multiple copies or LV.miR-125.T. We intercrossed the different founders and then analysed the F1 generation. In all analysed mice (n>30), we found reliable GFP expression and there were no differences in the pattern of GFP expression between different mice.

For vector injections into pups, 1 µl of concentrated lentiviral vector was unilaterally injected into the right ventricle of wild-type NMRI-mice or miR-125.T-mice at postnatal day 3 (P3) (males and females, Charles River). The pups were placed on ice for 5 minutes prior to positioning them in an ice-cold stereotaxic frame. Coordinates from lambda: AP +2.3, ML −0.8, DV −2.4.

For vector injections into the rostral migratory stream (RMS), 1 µl of concentrated lentiviral vector was unilaterally injected into the right RMS of wild-type 8-week-old C57BL/6-mice (females, Charles River). Coordinates from bregma: AP +3.3, ML −0.8, DV −2.9.

A proportion of the animals were given an intra-peritoneal pulse of 50 mg/kg BrdU (Sigma).

Odour stimulation

Mice were exposed to a cocktail of odours (Carlén et al., 2002) for 30 minutes, 21 days after virus (LV.miR-125.sp/LV.GFP) injection into the RMS. The mice were placed in an empty, open cage in the absence of food and water, in a fume hood with constant airflow. The mice were perfused immediately after odour exposure and immunohistochemistry for Fos was used to assess the immediate-early gene response.

Immunofluorescence

Mice were transcardially perfused with 4% paraformaldehyde (PFA) (Sigma), the brains post-fixed for 2 hours and transferred to phosphate-buffered saline (PBS) with 25% sucrose. Brains were coronally or sagittally sectioned on a microtome (35 µm) and put in KPBS.

Standard immunohistochemistry was used, as published in detail elsewhere (Sachdeva et al., 2010; Thompson et al., 2005). Primary antibodies were diluted as follows: chicken anti-GFP (1:1000; Abcam, GFP # Ab13970), mouse anti-NeuN (1:1000; Millipore, NeuN # MAb377), rabbit anti-GAD67 (1:5000; Chemicon, GAD67 # AB1511), rabbit anti-TH (1:1000, Pelfreeze, TH # P40101-0), goat anti-calretinin (1:2500, Millipore, Calretinin # MAb305), mouse anti-calbindin (1:1000; Sigma, Calbindin # C9848), mouse anti-parvalbumin (1:1000; Sigma, Parvalbumin # P3088) and rabbit anti-Fos (1:1000; Oncogene, c-Fos # PC05). The dilution factor of the secondary antibodies was 1:500 (Molecular Probes) or 1:200 (Jackson Laboratories).

For BrdU staining, the slices were fixed for 20 minutes in 4% PFA followed by incubation at 65°C in 1 M HCl before adding the primary antibody (1:500 rat anti-BrdU, Serotec).

Fluorescent *in situ* hybridisation

LNA-FISH was performed as previously described (Åkerblom et al., 2012). The slides were hybridised with a DIG-labelled miR-125b probe (Exiqon) diluted 1:200 for 1 hour at 61°C. The anti-DIG antibody was diluted 1:100 (Roche).

Quantification of GFP expressing cells in the OB

Two or three representative OB sections (35 µm) from each LV-injected animal were used for quantification (miR-125.T, n=5; LV.GFP, n=9; LV.miR-125.sp, n=12). Fluorescent images of GFP expression were taken with the same exposure and all GFP-expressing cells of the sections counted. The OB was divided into different cell layers based on DAPI staining, including the granule cell layer (GCL), mitral cell layer (MCL), external plexiform layer (EPL) and the glomerular layer (GL). The GCL was in turn divided into three equal cellular layers: the inner, middle and outer layer (iGCL, mGCL and oGCL, respectively). An unpaired t-test was performed in order to test for statistical significance. Data are presented as mean±s.e.m.

A z-stack of representative cells in the OB GCL from LV.GFP- (n=4) and LV.miR-125.sp- (n=4) injected mice was captured at 40× and cell morphologies (LV.GFP, n=10; LV.miR-125.sp, n=11) was investigated by measuring the length of the dendrites and counting the number of branch-points in the dendritic tree, using Canvas X, version 10.6.8. 100× z-stacks from the same material were used to count GC spine density (spines/µm) on the distal dendrites, here presented as percentage of control. An unpaired t-test was performed in order to test for statistical significance. Data are presented as mean±s.e.m.

Quantification of Fos/GFP/NeuN in the OB

6 OB-sections from LV.GFP and 6 OB-sections from LV.miR.125.sp RMS-injected mice were used for quantification. Three or four images were captured from each OB section and more than 500 NeuN-positive cells were counted/section. In total over 4000 NeuN-expressing cells were analysed in each group (LV.GFP/LV.miR-125.sp). Fos/NeuN- and Fos/GFP-expressing cells was identified using confocal microscopy. The GFP counts were normalised to the density of Fos expression in order to avoid a biased analysis due to uneven distribution of Fos in different sections. An unpaired t-test was performed in order to test for statistical significance. Data are presented as mean±s.e.m.

LNA-quantitative real-time PCR

Total RNA, including miRNA, was extracted from homogenised brain tissue using the miRNeasy kit (Qiagen) followed by Universal cDNA synthesis kit (Exiqon). LNA PCR primer sets, hsa-miR-125a, hsa-miR-125b and hsa-miR-124 (normalisation miRNA), were purchased from Exiqon and used together with LightCycler 480 SYBR Green I Master (Roche). Standard procedures for qRT-PCR were used and data quantified using the ΔΔCt-method.

qRT-PCR

Total RNA extraction was performed using the RNeasy Mini Kit (Qiagen). For RT-PCR, 1.5 µg of RNA was used for the reverse transcription performed with random primers (Invitrogen) and Superscript II (Invitrogen) according to supplier's recommendations. SYBR green qRT-PCR was performed as previously described. Data were quantified using the ΔΔCt-method and were normalised to Gapdh and β-actin expression. Primers were designed using Primer3 software (http://bioinfo.ut.ee/primer3-0.4.0). Primer sequences are found in supplementary material Table S3.

Gene ontology analysis

We extracted 594 target genes from the P13 mouse brain HITS-CLIP data set from Chi et al. (Chi et al., 2009). Out of these, we selected 251 with binding sites in 3′UTR. Two-hundred and thirty seven of these were successfully included into the DAVID bioinformatics database analysis. Using medium default stringency, we identified Gene Ontology biological process classes enriched in the miR-125 targets (Huang et al., 2009).

Luciferase reporter assay

A 591 bp sequence incorporating the miR-125 binding site in the Map3k1 3′UTR was amplified from mouse genomic DNA and cloned in the dual luciferase reporter vector pSICHECK-2 (Promega). The luciferase reporter construct was co-transfected with miR-125 and miR-124 overexpression constructs (Åkerblom et al., 2012) into 293 cells using Turbofect (Fermentas). Forty-eight hours after transfection, cells were assayed for luciferase activity using a dual-luciferase assay (Promega). One-way ANOVA followed by a Tukey's multiple comparison post-hoc test was performed in order to test for statistical significance. Data are presented as mean±s.e.m.

Acknowledgements

We are grateful to A. Björklund, M. Parmar, D. Trono, A Gritti and L. Naldini for providing reagents, and for stimulating discussions; and to S. Verp and I. Barde at the EPFL core facility for lentiviral transgenesis. We also thank U. Jarl, A. Josefsson, C. Isaksson, I. Nilsson, S. Smiljanic, A.-K. Oldén, E. Ling and M. Sparrenius for technical assistance.

Competing interests

The authors declare no competing financial interests.

Author contributions

M.Å., R.P., R.S., T.K. and B.M. designed and performed research and analysed data. B.G. contributed reagents. J.J. designed and coordinated the project and analysed data. M.Å. and J.J. wrote the paper.

Funding

This study was supported by grants from Swedish Research Council, The Swedish Cancer Foundation and the Basal Ganglia Disorders Linnaeus Consortium supported by Vetenskapsrådet. Deposited in PMC for immediate release.

Supplementary material

Supplementary material available online at
http://dev.biologists.org/lookup/suppl/doi:10.1242/dev.101659/-/DC1

References

Åkerblom, M., Sachdeva, R., Barde, I., Verp, S., Gentner, B., Trono, D. and Jakobsson, J. (2012). MicroRNA-124 is a subventricular zone neuronal fate determinant. *J. Neurosci.* **32**, 8879-8889.

Åkerblom, M., Sachdeva, R., Quintino, L., Wettergren, E. E., Chapman, K. Z., Manfre, G., Lindvall, O., Lundberg, C. and Jakobsson, J. (2013). Visualization and genetic modification of resident brain microglia using lentiviral vectors regulated by microRNA-9. *Nat. Commun.* **4**, 1770.

Alonso, M., Lepousez, G., Sebastien, W., Bardy, C., Gabellec, M. M., Torquet, N. and Lledo, P. M. (2012). Activation of adult-born neurons facilitates learning and memory. *Nat. Neurosci.* **15**, 897-904.

Batista-Brito, R., Close, J., Machold, R. and Fishell, G. (2008). The distinct temporal origins of olfactory bulb interneuron subtypes. *J. Neurosci.* **28**, 3966-3975.

Belluzzi, O., Benedusi, M., Ackman, J. and LoTurco, J. J. (2003). Electrophysiological differentiation of new neurons in the olfactory bulb. *J. Neurosci.* **23**, 10411-10418.

Boissart, C., Nissan, X., Giraud-Triboult, K., Peschanski, M. and Benchoua, A. (2012). miR-125 potentiates early neural specification of human embryonic stem cells. *Development* **139**, 1247-1257.

Brown, B. D., Gentner, B., Cantore, A., Colleoni, S., Amendola, M., Zingale, A., Baccarini, A., Lazzari, G., Galli, C. and Naldini, L. (2007). Endogenous microRNA can be broadly exploited to regulate transgene expression according to tissue, lineage and differentiation state. *Nat. Biotechnol.* **25**, 1457-1467.

Carlén, M., Cassidy, R. M., Brismar, H., Smith, G. A., Enquist, L. W. and Frisén, J. (2002). Functional integration of adult-born neurons. *Curr. Biol.* **12**, 606-608.

Chi, S. W., Zang, J. B., Mele, A. and Darnell, R. B. (2009). Argonaute HITS-CLIP decodes microRNA-mRNA interaction maps. *Nature* **460**, 479-486.

David, L. S., Schachner, M. and Saghatelyan, A. (2013). The extracellular matrix glycoprotein tenascin-R affects adult but not developmental neurogenesis in the olfactory bulb. *J. Neurosci.* **33**, 10324-10339.

De Marchis, S., Fasolo, A. and Puche, A. C. (2004). Subventricular zone-derived neuronal progenitors migrate into the subcortical forebrain of postnatal mice. *J. Comp. Neurol.* **476**, 290-300.

Doetsch, F., Caillé, I., Lim, D. A., García-Verdugo, J. M. and Alvarez-Buylla, A. (1999). Subventricular zone astrocytes are neural stem cells in the adult mammalian brain. *Cell* **97**, 703-716.

Edbauer, D., Neilson, J. R., Foster, K. A., Wang, C. F., Seeburg, D. P., Batterton, M. N., Tada, T., Dolan, B. M., Sharp, P. A. and Sheng, M. (2010). Regulation of synaptic structure and function by FMRP-associated microRNAs miR-125b and miR-132. *Neuron* **65**, 373-384.

Georgievska, B., Jakobsson, J., Persson, E., Ericson, C., Kirik, D. and Lundberg, C. (2004). Regulated delivery of glial cell line-derived neurotrophic factor into rat striatum, using a tetracycline-dependent lentiviral vector. *Hum. Gene Ther.* **15**, 934-944.

Gheusi, G., Lepousez, G. and Lledo, P. M. (2013). Adult-born neurons in the olfactory bulb: integration and functional consequences. *Curr. Top. Behav. Neurosci.* **15**, 49-72.

Hansen, T. B., Jensen, T. I., Clausen, B. H., Bramsen, J. B., Finsen, B., Damgaard, C. K. and Kjems, J. (2013). Natural RNA circles function as efficient microRNA sponges. *Nature* **495**, 384-388.

Huang, W., Sherman, B. T. and Lempicki, R. A. (2009). Systematic and integrative analysis of large gene lists using DAVID bioinformatics resources. *Nat. Protoc.* **4**, 44-57.

Imayoshi, I., Sakamoto, M., Ohtsuka, T., Takao, K., Miyakawa, T., Yamaguchi, M., Mori, K., Ikeda, T., Itohara, S. and Kageyama, R. (2008). Roles of continuous neurogenesis in the structural and functional integrity of the adult forebrain. *Nat. Neurosci.* **11**, 1153-1161.

Lagos-Quintana, M., Rauhut, R., Yalcin, A., Meyer, J., Lendeckel, W. and Tuschl, T. (2002). Identification of tissue-specific microRNAs from mouse. *Curr. Biol.* **12**, 735-739.

Le, M. T., Xie, H., Zhou, B., Chia, P. H., Rizk, P., Um, M., Udolph, G., Yang, H., Lim, B. and Lodish, H. F. (2009). MicroRNA-125b promotes neuronal differentiation in human cells by repressing multiple targets. *Mol. Cell. Biol.* **29**, 5290-5305.

Lee, R. C., Feinbaum, R. L. and Ambros, V. (1993). The C. elegans heterochronic gene lin-4 encodes small RNAs with antisense complementarity to lin-14. *Cell* **75**, 843-854.

Lemasson, M., Saghatelyan, A., Olivo-Marin, J. C. and Lledo, P. M. (2005). Neonatal and adult neurogenesis provide two distinct populations of newborn neurons to the mouse olfactory bulb. *J. Neurosci.* **25**, 6816-6825.

Magavi, S. S., Mitchell, B. D., Szentirmai, O., Carter, B. S. and Macklis, J. D. (2005). Adult-born and preexisting olfactory granule neurons undergo distinct experience-dependent modifications of their olfactory responses in vivo. *J. Neurosci.* **25**, 10729-10739.

Sachdeva, R., Jönsson, M. E., Nelander, J., Kirkeby, A., Guibentif, C., Gentner, B., Naldini, L., Björklund, A., Parmar, M. and Jakobsson, J. (2010). Tracking differentiating neural progenitors in pluripotent cultures using microRNA-regulated lentiviral vectors. *Proc. Natl. Acad. Sci. USA* **107**, 11602-11607.

Sauvain, M. O., Dorr, A. P., Stevenson, B., Quazzola, A., Naef, F., Wiznerowicz, M., Schütz, F., Jongeneel, V., Duboule, D., Spitz, F. et al. (2008). Genotypic features of lentivirus transgenic mice. *J. Virol.* **82**, 7111-7119.

Thompson, L., Barraud, P., Andersson, E., Kirik, D. and Björklund, A. (2005). Identification of dopaminergic neurons of nigral and ventral tegmental area subtypes in grafts of fetal ventral mesencephalon based on cell morphology, protein expression, and efferent projections. *J. Neurosci.* **25**, 6467-6477.

Vergaño-Vera, E., Yusta-Boyo, M. J., de Castro, F., Bernad, A., de Pablo, F. and Vicario-Abejón, C. (2006). Generation of GABAergic and dopaminergic interneurons from endogenous embryonic olfactory bulb precursor cells. *Development* **133**, 4367-4379.

Wightman, B., Ha, I. and Ruvkun, G. (1993). Posttranscriptional regulation of the heterochronic gene lin-14 by lin-4 mediates temporal pattern formation in C. elegans. *Cell* **75**, 855-862.

Zufferey, R., Nagy, D., Mandel, R. J., Naldini, L. and Trono, D. (1997). Multiply attenuated lentiviral vector achieves efficient gene delivery in vivo. *Nat. Biotechnol.* **15**, 871-875.